



Impact of commercial cooking on urban PM_{2.5} and O₃ with online data-assisted emission inventory



Yingzhi Yuan^a, Yun Zhu^{a,*}, Che-Jen Lin^b, Shuxiao Wang^{c,d}, Yanghong Xie^e, Haixian Li^e, Jia Xing^{c,d}, Bin Zhao^{c,d}, Mengmeng Zhang^a, Zhiqiang You^a

^a Guangdong Provincial Key Laboratory of Atmospheric Environment and Pollution Control, College of Environment and Energy, South China University of Technology, Guangzhou Higher Education Mega Center, Guangzhou 510006, China

^b Department of Civil and Environmental Engineering, Lamar University, Beaumont, TX 77710, USA

^c State Key Joint Laboratory of Environment Simulation and Pollution Control, School of Environment, Tsinghua University, Beijing 100084, China

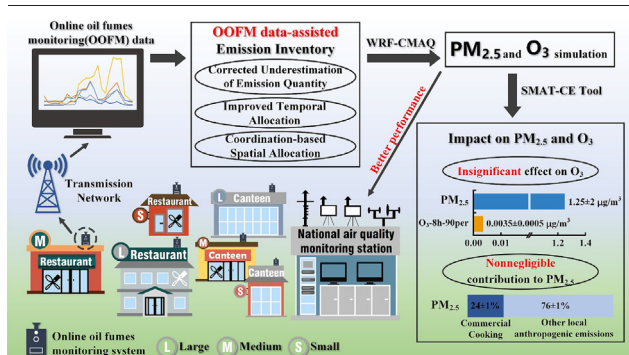
^d State Environmental Protection Key Laboratory of Sources and Control of Air Pollution Complex, Beijing 100084, China

^e Shunde Branch of Foshan Ecological Environment Bureau, Foshan 528000, China

HIGHLIGHTS

- A novel approach to develop spatiotemporally resolved emission inventory from commercial cooking.
- Temporal emission characteristics of restaurants and canteens were first discovered.
- Model performance of PM_{2.5} and O₃ simulation was improved with the new inventory.
- Impact of commercial cooking on PM_{2.5} and O₃ was assessed in an urban district of China.
- Targeted control measures in areas with high commercial cooking density will lower ambient PM_{2.5}.

GRAPHICAL ABSTRACT



ARTICLE INFO

Editor: Hai Guo

Keywords:

Commercial cooking
Online oil fumes monitoring data
Emission inventory
Air quality modeling
Impact assessment

ABSTRACT

Commercial cooking (CC) is an intensive near-field source contributing to ambient PM_{2.5} and O₃ concentration in urban areas. Compilation of CC emission inventory has been challenging due to the dynamic variation of the emission sector, which has resulted in data deficiencies including underestimated quantity and poor temporal-spatial resolution. In this study, we have developed a methodology that integrates existing emission statistics with online oil fumes monitoring (OOFM) data to create a highly spatiotemporally resolved emission inventory of CC. The new emission estimate differs from legacy inventory in emission quantity and temporal pattern. Using the emission data, the impacts of CC emission on local PM_{2.5} and O₃ were evaluated using WRF-CMAQ and model-monitor data fusion tool of SMAT-CE in Shunde, China. The OOFM data-assisted emission inventory led to improved model performance for both model-predicted PM_{2.5} and O₃ concentrations. The simulation results using the new inventory data showed that the CC emissions contributed 1.25 ± 2 μg/m³ of PM_{2.5}, and accounted for 24 ± 1% of PM_{2.5} concentration derived from local anthropogenic emissions. Moreover, a higher contribution of CC to PM_{2.5} was predicted in areas with elevated CC emissions, while the contribution to O₃ was insignificant.

* Corresponding author.

E-mail address: zhuyun@scut.edu.cn (Y. Zhu).

1. Introduction

In recent years, atmospheric pollution caused by fine particulate matter (PM_{2.5}) and ground-ozone (O₃) (Burnett et al., 2018; Lu et al., 2020) has drawn scientific attention worldwide due to their negative influence on air quality and human health (Burnett et al., 2018; Xiao et al., 2022). With the effective implementation of control policies for major pollution sources (e.g., industry, dust and transportation) (Yu et al., 2019; Zhou et al., 2020; Zhu et al., 2019), the annual PM_{2.5} concentration in China decreased sharply by 30.56 % between 2013 and 2015. However, the declining trend has slowed down significantly (Clean Air Asia, 2021; Tan and Mao, 2021) since 2016 with an average annual decline of <10 % (Fig. S1), and the O₃ levels have shown a rising trend particularly in many megacities in summer (Li et al., 2020a; Li et al., 2020b). In support of further mitigating PM_{2.5} and O₃ pollution, except for the major sources, it has been proposed to strengthen control of residential emission sources from national to local scale. As one of the most important residential sources, cooking oil fumes (COF) is a complex mixture of PM_{2.5}, volatile organic compounds (VOCs) and other carcinogens (Kabir and Kim, 2011; Lu et al., 2021; Xu et al., 2020), which makes it an intensive contributor to the ambient PM (ElSharkawy and Ibrahim, 2022; Robinson et al., 2018) as well as O₃ (He et al., 2020; King et al., 2021). Commercial cooking activities, a major contributor to COF, emitted higher concentration levels and more complex components of COF than that of family cooking (Lu et al., 2019; Sun et al., 2022). Thus, revealing the emission characteristic of commercial cooking and associated impact on both PM_{2.5} and O₃ is critical for pollution regulatory management.

A high-resolution and constantly updated emission inventory plays an important role in assessing the impact of emission sources on ambient air quality (Crabbe et al., 1999; Kurokawa and Ohara, 2020). Currently, the development of commercial cooking emission inventories mainly relies on the activity levels from annual statistical data, technical manuals (e.g. *Technical manual for the preparation of city-level air pollutant emission inventory 2017*), or surveys (Jin et al., 2021; Liang et al., 2022; Wang et al., 2018), which had a long data renewal period and thus failed to reflect the fast-changing emission pattern caused by the rapid growth of catering industry (Yu et al., 2020). Besides, detailed temporal-spatial distribution data were seldom provided, causing difficulty in the emission variability analysis (Liu et al., 2018a) and regional air quality modeling (Sturm et al., 1999). These shortcomings make challenges in improving the accuracy of cooking emission inventory and accordingly limit its application in quantifying the impact on ambient air quality. Various kinds of online monitoring data, which can offer real-time emission information and capture detailed emission characteristics, have been widely used to estimate emissions from other sources (Sun et al., 2021; Yang et al., 2021; Zhang et al., 2018). However, similar data have not been applied to compile commercial cooking emission inventory. In addition, previous studies of commercial cooking impact assessment were mainly concentrated on indoor air quality (Kang et al., 2019; Lee et al., 2001; Militello-Hourigan and Miller, 2018; Seaman et al., 2009), whereas less attention has been paid to outdoor air quality. Our understanding of the commercial cooking impact on the surrounding environment was currently limited to its contribution to the atmospheric organic aerosol (Liu et al., 2018b; Siouti et al., 2021; Zhang et al., 2021), lacking further research on both PM_{2.5} and O₃.

In this study, a high temporal-spatial resolution emission inventory of commercial cooking was firstly developed based on the realistic activity levels adopted from the online oil fumes monitoring (OOFM) system in Shunde, a famous gastronomic district with developed catering industries in the Pearl River Delta (PRD) region, China. Then the coupled modeling system of the Weather Research and Forecasting (WRF) model and Community Multiscale Air Quality (CMAQ) model was applied to verify the accuracy of the emission inventory. The tool for Model Attainment Test: Community Edition (SMAT-CE) (Li et al., 2019), together with the air pollutants monitoring data, was subsequently used to fuse the simulation results to explore the impact of commercial cooking on ambient PM_{2.5} and O₃. The method and the results of this study will be beneficial to

understanding the emission characteristic of commercial cooking and further provide a scientific basis for its pollution control.

2. Materials and methods

The technical scheme of this study was shown in Fig. 1. Firstly, the emissions quantity was estimated by improving the activity level dataset that involved stove heads, working hours and oil fumes gas discharge rate. The above activity levels were obtained from field investigation and OOFM data which had been screened based on a well-known anomaly recognition method named Pauta Criterion (3 sigma criterion). Secondly, the total emissions were spatially allocated according to the real location of each restaurant and canteen and then temporally allocated with the hourly coefficient from OOFM data to obtain a high-resolution emission inventory (EI_{on}). Besides, a legacy emission inventory (EI_{le}) was also compiled based on the 2018 Shunde statistical data and *Technical manual for the preparation of city-level air pollutant emission inventory 2017 (Technical Manual)*. Thirdly, the WRF-CMAQ platform was utilized to verify the accuracy of EI_{on} by comparing the simulation results of EI_{on} and EI_{le}. Finally, the simulation result of EI_{on} was fused with the monitoring data through the SMAT-CE Tool (Huang et al., 2018) to better quantify the impact of commercial cooking on ambient PM_{2.5} and O₃.

2.1. Online oil fumes monitoring system of commercial cooking and data screening

The OOFM system, recently popularized in restaurants and canteens in the developed cities of China, was utilized to automatically detect the concentration of cooking emissions and monitor the operational status of purification equipment and wind turbines 24 h a day. Detailed operation process and hardware of the OOFM system were given in Section S1 and Figs. S2 to S4. The OOFM data including monitoring time, operation status of both purification equipment and wind turbines, and oil fumes concentration per 10 min for 89 restaurants and 13 canteens in 2018 were collected. In order to ensure the reliability of monitoring data, regular maintenance of the monitoring system and cleaning of the detector were scheduled to guarantee the normal operation of various components (Fig. S5). The flow velocity in the exhaust duct was also measured 2–3 times by using calibrated pitot tubes flowmeter (LOBO, type LB-60) after each maintenance for further calculation of oil fumes gas discharge rate. Besides, the screening of monitoring data was performed to ensure reliability before their application in emissions calculation. First, the detected data, corresponding to the system operation status shown as unavailable (NA) and shutdown, were excluded. Then, the oil fumes concentration data detected during system operation and shutdown was separately filtered based on the Pauta Criterion (Li et al., 2020c; Liu et al., 2018c; Zhao et al., 2018). Data that deviated more/<3-fold standard from the mean were removed, and the corresponding information including switching state and operating current of purification equipment and wind turbines were also removed.

2.2. Development of emission inventories without and with online oil fumes monitoring data

A legacy emission inventory (EI_{le}) including VOCs, PM_{2.5}, PM₁₀, black carbon (BC) and organic carbon (OC) emissions of commercial cooking for 2018 in Shunde was developed based on the *Technical Manual* without OOFM data. The calculation method of annual emissions was given in Section S2. The emissions were spatially allocated into grid cells with a horizontal resolution of 1 km × 1 km according to the population distribution. The temporal allocation was performed by referring to the hourly and daily coefficients in the *Technical Manual*; monthly coefficients were assumed the same (1 divided by 12, 0.083) for each month since referable values were not provided in the *Technical Manual*.

The emission inventory of commercial cooking incorporating OOFM data (EI_{on}) was established using a bottom-up method. Except for the OOFM data mentioned in Section 2.1, the activity levels were also taken

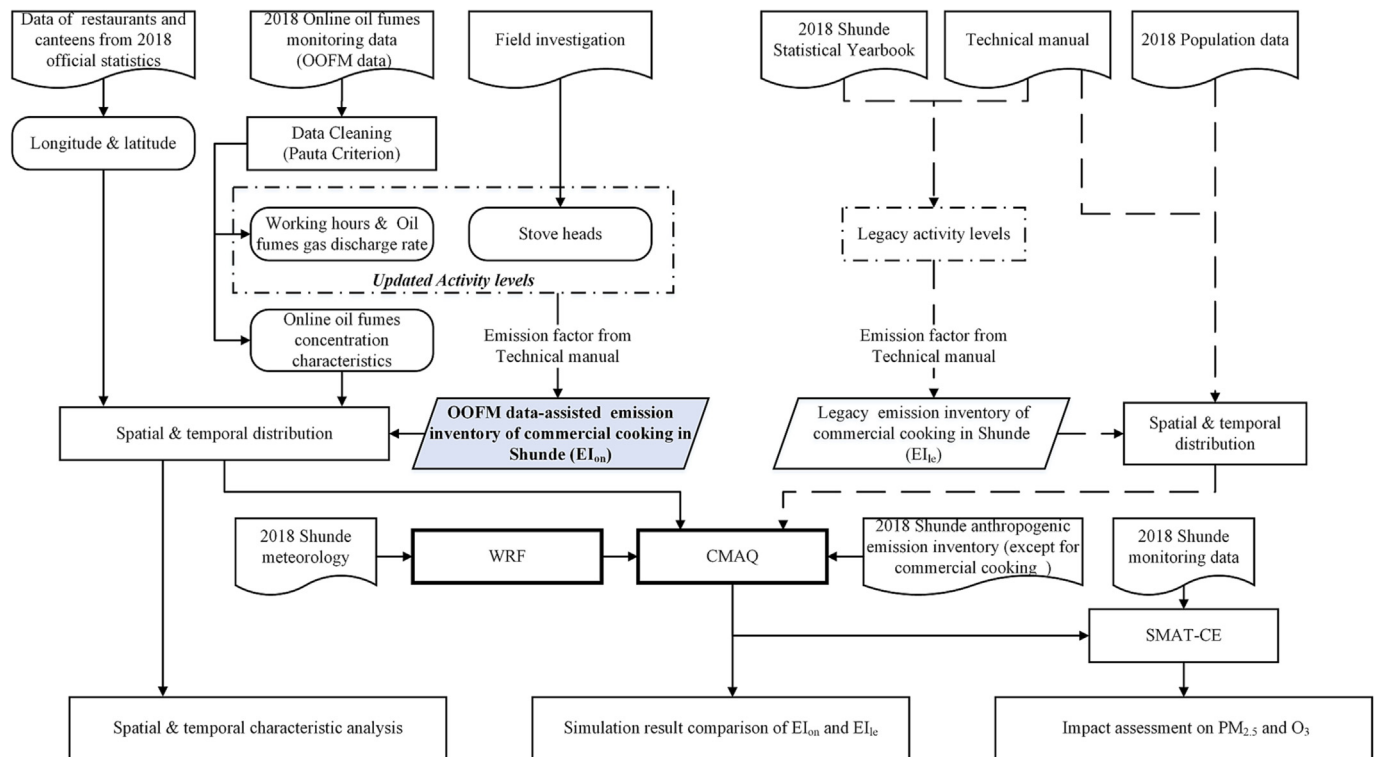


Fig. 1. The technical scheme for impact assessment of commercial cooking on PM_{2.5} and O₃ with online data-assisted emission inventory.

from official statistical data and field investigations. Basic information, including unit name, location, seating capacity, business type, business scope, business registration status, date of establishment and date of latest business status change of all the restaurants and canteens in Shunde district, was obtained from the official statistical data. The scale of each restaurant or canteen was classified by its seating capacity (≤ 75 , 76–250 and ≥ 251 correspond to small, medium and large business scales, respectively) (Guangdong Food and Drug Administration, 2010). A field investigation was conducted on 397 typical restaurants selected in proportion to restaurant scales as well as all the canteens to assess important information including stove heads, installation and maintenance of purification equipment. Significantly, the restaurants and canteens with OOFM systems were also investigated. The sample size of investigated restaurants could make the anticipation error $< 5\%$ under the premise of 95% confidence interval, which met the statistical requirements (Wang and Ji, 2020). Specific values of activity levels were shown in Table S1.

The annual commercial cooking emission estimations were made following Eq. (1). The removal efficiency of oil fumes was not adopted in this study: on the one hand, there was a lack of effective purification equipment in most small restaurants according to our investigation (Table S1); on the other hand, the lack of regular cleaning and maintenance of installed purification equipment (Fig. S6, Table S1) was widespread in most large and medium restaurants, resulting in the significant decline of removal efficiency in the real world (Lin et al., 2021).

$$E_i = \sum_n EF_i \times N_n \times V_n \times T_n \times 10^{-9} \quad (1)$$

where,

i is one of the five pollutants (VOCs, PM_{2.5}, PM₁₀, BC and OC).

n is the total number of restaurants/canteens.

E is the emissions (t/a) of pollutant i .

EF is the emission factor (mg/m³) for five pollutants of cooking listed in the *Technical Manual*. The values were 5.60, 6.40, 8, 0.13 and 4.48 for VOCs, PM_{2.5}, PM₁₀, BC and OC, respectively.

N is the number of stove heads. For investigated restaurants/canteens, the N values were their actual number of stove heads. For those uninvestigated restaurants/canteens with large, medium and small scales, respectively, the N values were represented by the averaged number of stove heads (Eq. (S2) in Section S3) corresponding to their self-business scales.

V is the oil fumes gas discharge rate of each stove head (m³/h). For restaurants/canteens with the OOFM system, the V values were obtained by dividing the measured oil fumes gas discharge rate by the number of stove heads (MDRSH) in each restaurant/canteen. For restaurants/canteens without OOFM system, the V values were represented by the averaged MDRSH (Eq. (S3) in Section S3) corresponding to their self-business scale (large, medium and small scale), respectively.

T is the annual working hours (h/a). For restaurants/canteens with OOFM system, the T values were the annual working hours of purification equipment of each restaurant/canteen in 2018. For restaurants/canteens without OOFM system, the T values were represented by the averaged working hours (Eq. (S4) in Section S3) corresponding to their self-business scale (large, medium and small scale), respectively.

Improving the accuracy of temporal and spatial distribution is favorable for reducing the uncertainty of the developed high-resolution emission inventory, thereafter improving the model performance. In this study, the commercial cooking emissions were spatially aggregated onto the grids with 1 km × 1 km resolution in accordance with the realistic geographic coordinate of restaurants and canteens. The monthly, daily (within a week) and hourly profiles were obtained from the oil fumes concentration in OOFM data and then applied to the temporal allocation of the gridded emissions. Taking monthly profile as an example, we processed the calculation of temporal profiles as the following three steps:

- (1) First, the monthly means for each restaurant/canteen with OOFM data were calculated based on its respective oil fumes concentration.
- (2) Then, the monthly means were standardized by normalization method (Liu et al., 2019) to eliminate magnitude differences among restaurants/canteens.
- (3) Last, the median value of the standardized monthly means in all the

restaurants/canteens with large, medium and small scales were introduced as the representative monthly coefficients of corresponding business-scale restaurants/canteens, respectively. For example, we chose the median value of the standardized January means in all large restaurants with OOFM data to represent the January coefficients for the large restaurants.

The same processes were also performed to obtain representative daily (within a week) and hourly coefficients of three business-scales restaurants/canteens.

2.3. WRF-CMAQ modeling

In this study, CMAQ model version 5.2 coupled with WRF model version 3.9.1 was applied to simulate the base concentration of ambient air pollutants. The WRF model was used to provide meteorological input for CMAQ model (Cheng et al., 2012). Four nested domains with grid resolutions of 27 km (d01), 9 km (d02), 3 km (d03) and 1 km (d04) were established for WRF-CMAQ modeling as shown in Fig. S7. All nesting domains were vertically divided into 14 layers with varying thicknesses. The d03 domain covered the entire Pearl River Delta (PRD), and the d04 domain focused on the Shunde district. The entire year of 2018 was selected as the simulation period. The emission inventories for the d01 and d02 domains were obtained from the Multi Resolution Emission Inventory for China (MEIC: <http://meicmodel.org>). The emission inventories for the d03 and d04 domains were developed by our research group; the commercial cooking emissions in Shunde district were made into a separate modeling input file, and were not included in the inventory of d04 domain (Table S2). The natural emissions for four nesting domains were acquired through the Model of Gases and Aerosols from Nature (MEGAN) version 2.10 (Guenther et al., 2012). The initial and boundary conditions for inner d02 and d03 domains were provided from the upper CMAQ simulation results. The PM_{2.5} and VOCs source profiles in this study were adopted from SPECIATE 5.2 database published by the U.S. Environmental Protection Agency (<https://www.epa.gov/air-emissions-modeling/speciate>). A 3-day spin-up period was performed to minimize the initial condition influences. Detailed options for WRF and CMAQ configurations were given in Table S3.

The relationship between simulated and observed data at air quality monitoring stations was constructed using the eVNA algorithm in the SMAT-CE Tool (<http://www.abacas-dss.com/abacas/Software.aspx>) (Li et al., 2019; Wang et al., 2015) and then applied to adjust the grid simulation result (Section S4). The observed data of six national air quality monitoring stations and eight local air quality monitoring stations (Fig. S7) were obtained from the Guangdong Environmental Quality platform (<http://113.108.142.147:20061/StationStatus/AppCheck>) and Shunde Branch of Foshan Municipal Ecology and Environment Bureau (<https://hycx-gd.cn/AqiShunDe/>), respectively. Case_{ie} and Case_{on}, two emission scenarios of commercial cooking estimated using *Technical Manual* and OOFM data, respectively, were compared to evaluate the model performance of the OOFM data-assisted emission inventory. In addition, we performed two zero-out scenarios where the all anthropogenic emissions (Case_{an}) and commercial cooking emissions in Shunde district (Case_{cc}) were turned off, respectively. The differences in the amended results by SMAT-CE Tool between these two zero-out and Case_{on} scenarios were quantified to represent the contribution of local commercial cooking emissions to ambient PM_{2.5} and O₃ (Eqs. S10 to S11 in Section S6).

3. Results and discussion

3.1. Emission inventories of commercial cooking

The legacy (EI_{ie}) and OOFM data-assisted (EI_{on}) emission inventories of commercial cooking in Shunde district for the year 2018 were summarized in Fig. 2(a). The annual emissions of VOCs, PM_{2.5}, PM₁₀, BC and OC

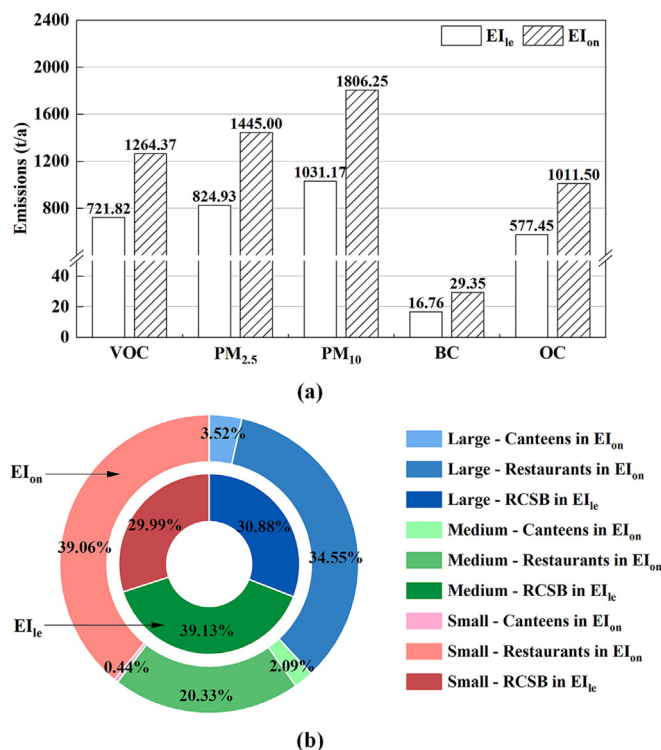


Fig. 2. (a) 2018 commercial cooking emissions from legacy (EI_{ie}) and OOFM data-assisted emission inventories (EI_{on}) in Shunde district, unit: ton/annually (t/a). (b) The outermost doughnut represented the proportion of VOCs emissions from large, medium and small restaurants and canteens in EI_{on}, and the innermost doughnut represented the proportion of VOCs emissions from large, medium and small registered catering service businesses (both restaurants and canteens, RCSB) in the EI_{ie}.

calculated with OOFM data were 1264.37 t, 1445.00 t, 1806.25 t, 29.35 t and 1011.50 t, respectively, which were nearly 1.75 times that of those from EI_{ie}. This increase was mostly attributed to the updated activity levels. As mentioned in Section 2.2, the real-world activity levels, including stove heads, working hours and oil fumes gas discharge rate, were collected separately from field investigation, OOFM data and in-situ measurement. It was found that the averages of the above three parameters for small, medium and large restaurants were 1.12–1.45 times larger than the recommended values in the *Technical Manual* (Table 1), respectively, which mainly came from the combined influence of well-developed catering

Table 1

The activity levels of different business scales restaurants and canteens for 2018 in EI_{ie} and EI_{on}.

	Scale	Proportion (%)	Stove heads	Working hours (h)	Oil fumes gas discharge rate (m ³ /h)	
EI _{on} ^a	Restaurants	Large	8.51	9.2	2464	2878
		Medium	14.68	4.7	2102	2245
		Small	76.81	2.2	1911	1962
	Canteens	Large	38.08	3.8	1649	2615
		Medium	46.11	1.9	2008	2142
		Small	15.81	1.7	1405	2074
Registered catering service businesses (both restaurants and canteens)	Large	7.30	7.1	2000	2500	
	Medium	22.80	4.0	1800	2000	
	Small	69.90	1.5	1600	1500	

^a EI_{ie} and EI_{on} were the legacy (EI_{ie}) and OOFM data-assisted emission inventories (EI_{on}) in Shunde district, respectively.

industry and rapid growth of take-out industry (Shangguan, 2019) in Shunde district.

Except for the activity levels, the distribution of business scales was also an important factor in emission estimations. Fig. 2(b) listed the proportion of VOCs emissions from large, medium and small restaurants and canteens in EI_{on} and registered catering service businesses in EI_{le} , respectively. The registered catering service businesses (RCSB) were the sum of restaurants and canteens. The emission distribution of three kinds of restaurants in EI_{on} was inconsistent with that in EI_{le} ; the VOCs emissions from small and medium restaurants were the highest and lowest in EI_{on} , respectively, while this was the opposite in EI_{le} . Compared with the available proportion of business scale for 2007 applied in EI_{le} , the ratio of small restaurants was significantly increased; this is because the development of the take-out industry led to the increase of small restaurants.

Considering the differences in cooking characteristics between canteens and restaurants, the emissions of canteens were considered separately from restaurants based on the realistic activity levels for the first time in EI_{on} . The emissions of VOCs, $PM_{2.5}$, PM_{10} , BC and OC from canteens were 76.52 t/a, 87.46 t/a, 109.33 t/a, 1.77 t/a and 61.23 t/a, respectively, accounting for nearly 6 % of those in EI_{on} . Notably, the scale distribution of canteens was completely different from that of restaurants; there were greater numbers of medium and large canteens and fewer small canteens. In addition, the average stove heads and working hours of canteens were generally lower than the recommended values in EI_{le} (Table 1). One exception is that the average working hours of medium canteens from OOFM data at 2008 h was higher than that from *Technical Manual* at 1800 h; this was because two (C9 and C10, Table S1) of the six medium canteens with OOFM data belong to the police station and hospital respectively with up to 24 working hours.

These results implied that the activity levels based on OOFM data and related statistical data were more favorable to capture the real-world emission characteristics of restaurants and canteens. For instance, compared with the unified working hours recommended in the *Technical Manual*, our statistics for large, medium and small restaurants all showed increasing trends, while that of small and large canteens decreased significantly. Obviously, calculating the emissions uniformly according to the recommended values would result in the overestimation of the canteens and underestimation of the restaurants, respectively, increasing the uncertainty of the estimations. Hence, developing the emission inventory based on realistic monitoring data is beneficial to improve the accuracy of emission estimations with more local characteristics, accordingly providing sound support for the development of targeted control measures.

3.2. Spatial and temporal characteristic analysis

Taking $PM_{2.5}$ as a representative pollutant, we illustrated the spatial distributions of restaurants and canteens emissions in EI_{on} with a resolution of $1 \text{ km} \times 1 \text{ km}$ in Fig. 3(b-c). In this study, owing to the updated spatial profiles based on the realistic coordinate, the gridded emissions manifested obvious spatial variability that more accurately reflected the real emissions pattern. Obviously, the emissions of VOCs and $PM_{2.5}$ from restaurants were spatially clustered, which was consistent with the pattern of recreational places (including shopping malls, chess rooms, teahouses, hair salons, theaters, etc., Fig. S8). The emissions of VOCs and $PM_{2.5}$ from canteens were concentrated in Ronggui and Daliang which were defined as the subsidiary administrative center with many institutions and schools, and those in the remaining eight towns were concentrated around local governments (Fig. S8). By comparison, the emissions of commercial cooking in the legacy version were allocated spatially using the population density as the gridding surrogates (Fig. 3(a)), and they failed to capture the hotspot since the population density was unable to reflect the extent where restaurants and canteens congregate accurately.

Fig. 4 illustrated the average monthly, daily (within a week) and hourly variations of commercial cooking for which temporal profiles were updated from the online oil fumes concentration. Overall, the updated temporal coefficients varied significantly with the recommended values in the *Technical Manual* except for daily (within a week) coefficients for restaurants, and there were also obvious differences in the temporal distribution between restaurants and canteens. As for the monthly distribution (Fig. 4(a)), the average monthly coefficients for restaurants in EI_{on} were distributed in the interval of 0.07–0.09, showing a relatively smooth monthly variation. In contrast, the monthly emissions of canteens varied considerably, with significant declines in February, July and August. One possible reason for this was the long vacation during the Spring Festival in February and the summer vacation in July and August of the school.

As for the daily distribution within the week (Fig. 4(b)), the average emissions of restaurants varied a little from Monday to Sunday, resembling that in the EI_{le} . However, significant fluctuation occurred in the emissions trend of canteens. More interestingly, the opposite weekend effect was demonstrated between restaurants and canteens, of which the emissions were increased slightly and sharp slump, respectively. Most canteens are located within schools and business buildings (e.g., schools, kindergartens and administrative institutions), and therefore have reduced emission over weekends.

As for the hourly distribution (Fig. 4(c)), the emissions of restaurants had a trimodal distribution with peaks at 10:00, 12:00 and 19:00 (Beijing time), while that in EI_{le} peaked at 7:00, 12:00 and 19:00 to 20:00 (Beijing time) and stayed stable in the remaining hours. The peak at 10:00 may be

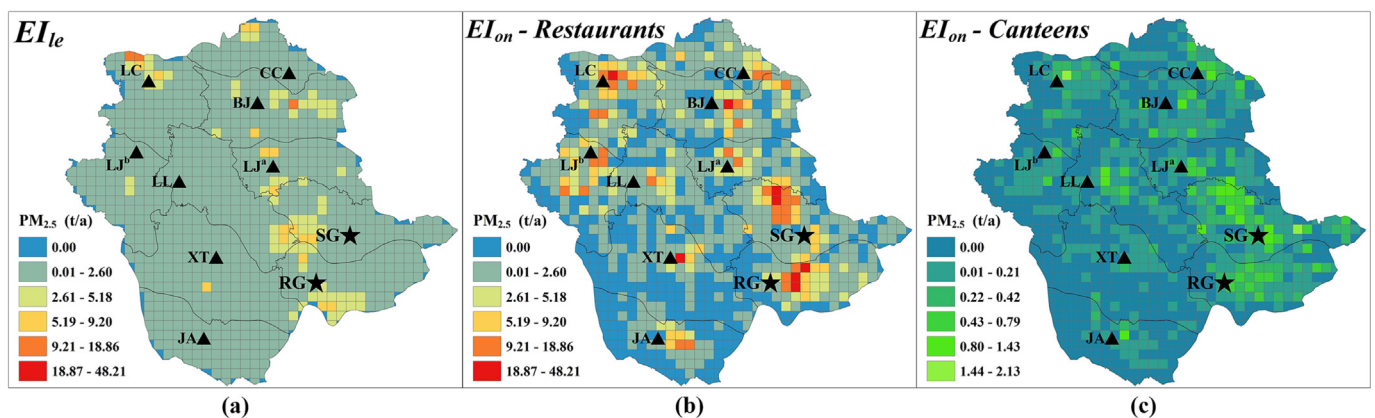


Fig. 3. (a): Population density-based spatial distributions of $PM_{2.5}$ emissions from registered catering service businesses (including restaurants and canteens) in EI_{le} . (b-c): Coordinate-based spatial distributions of $PM_{2.5}$ emissions from restaurants and canteens in EI_{on} . The black five-pointed stars represented the national air quality monitoring stations. RG: Ronggui, SG: Sugang. The black triangles represented local air quality monitoring stations. JA: Junan, XT: Xingtian, LL: Leliu, LJ^a: Lunjiao, LJ^b: Longjiang, BJ: Beijiao, LC: Lecong, CC: Chencun.

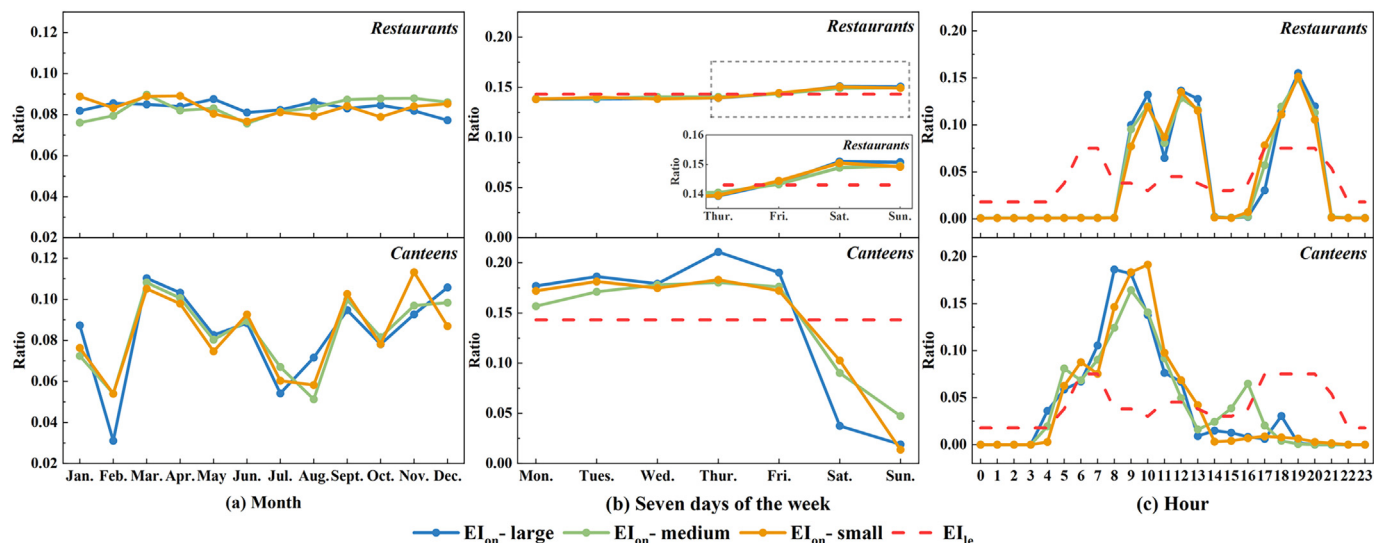


Fig. 4. Monthly (a), daily (within a week) (b) and hourly (c) temporal coefficients calculated based on the OOFM data for three types (large, medium and small) of restaurants and canteens. The temporal profiles of EI_e were obtained from the *Technical Manual*, where the legacy monthly profiles were not provided.

attributed to the fact that restaurants need to prepare in advance to meet the high consumer demand at lunchtime (12:00, Beijing time). Compared with that in restaurants, the average hourly emissions from large, medium and small canteens peak earlier at 8:00, 9:00 and 10:00 (Beijing time), respectively. Because the cooking in canteen should be completed ahead to facilitate the internal staff and students dining on time.

These results illustrated strong spatial and temporal variabilities of commercial cooking emissions across spatial and multi-scale temporal allocation. The restaurant emissions were concentrated in the areas with high density of urban activities. As to the temporal allocation, the low emissions of canteens during summer and winter vacation, the opposite weekend emission effect between restaurants and canteens and the beforehand emissions in the morning of both restaurants and canteens were captured and first reported assisted with the OOFM concentration. The hourly variabilities during peak hours were underestimated by the legacy values in *Technical Manual*, while the weekend variabilities of canteens were significantly overestimated. Thereout, the coordination-based spatial allocation and OOFM concentration-assisted temporal allocation were conducive to reveal more detailed spatial-temporal emission patterns of commercial cooking, improving the estimation accuracy of spatial and temporal emissions.

3.3. Comparison of the simulation result based on legacy and OOFM data-assisted emission inventories

The WRF-CMAQ modeling system was utilized to simulate the ambient O_3 and $PM_{2.5}$ concentrations based on the legacy and OOFM data-assisted emission inventories, respectively. To evaluate the model performance, the original simulation results from the WRF-CMAQ modeling system of $Case_{le}$ and $Case_{on}$ were compared with O_3 and $PM_{2.5}$ monitoring data in two national air quality monitoring stations (NAQMS) located in the emission-updated areas, Ronggui (RG) and Sugang (SG). The descriptions of statistical indicators including normalized mean bias (NMB) and correlation coefficient (R) and associated evaluation results were given in Section S5 and Tables S4 to S5, respectively. The verification of time series was driven by the simulation of $Case_{on}$ and the monitoring data as demonstrated in Figs. S9 to S10.

Overall, the EI_{on} -based modeling system was more performable in the $PM_{2.5}$ and O_3 simulation at two stations. Taking SG as an example, although the $PM_{2.5}$ simulation in both $Case_{on}$ (modeling study based on the EI_{on}) and $Case_{le}$ (modeling study based on EI_e) showed a positive correlation (monthly $R > 0.41$) with observations, the monthly R values in $Case_{on}$ were slightly higher than that in $Case_{le}$, indicating that the hourly variations were more reasonably captured by the EI_{on} -based modeling system.

The NMB values for $PM_{2.5}$ in these two cases ranged from -12.17% to 9.35% , meeting the criteria ($NMB \leq \pm 15\%$) recommended by U.S. Environmental Protection Agency et al. (2007). Notably, both these two cases showed underestimation for $PM_{2.5}$ simulation in months except February and December, but the underestimation was slightly lower in $Case_{on}$ than that in $Case_{le}$. This is because the elevated $PM_{2.5}$ concentrations caused by the increased $PM_{2.5}$ emission from commercial cooking in emission-updated areas were considered in $Case_{on}$.

The high R and negative NMB for O_3 simulation were found in both $Case_{on}$ and $Case_{le}$, indicating the simulated O_3 time series was acceptable but underestimated overall, especially at night. Differing from that for $PM_{2.5}$ simulation, the discrepancies between the modeling performance in $Case_{on}$ and $Case_{le}$ were relatively smaller for O_3 , implying the improvement of EI_{on} in O_3 simulation was less obvious than that in $PM_{2.5}$ simulation. One major reason is that the regional emissions and intraregional transport played an important role in O_3 formation in Shunde district (Fang et al., 2021; Yang et al., 2019), while the local precursor emissions including either commercial cooking or other important sources had a much smaller influence on ambient O_3 . In general, the simulated $PM_{2.5}$ and O_3 in $Case_{on}$ were closer to observations by updating the magnitudes and temporal-spatial characteristics of local commercial cooking emissions in EI_{on} .

3.4. Impact assessment of commercial cooking on $PM_{2.5}$ and O_3

Exploring the impact of commercial cooking on the ambient atmospheric environment is conducive to air pollution control. The contribution of commercial cooking to ambient $PM_{2.5}$ and O_3 at RG and SG (Fig. 5) was calculated as the differences in amended $PM_{2.5}$ and 90th percentile of the daily maximum 8-h average O_3 (O_3 -8h-90per) concentrations that driven from the SMAT-CE Tool between $Case_{on}$ and $Case_{cc}$, representing the reduction of $PM_{2.5}$ and O_3 -8h-90per concentration by eliminating local commercial cooking emissions. The contribution proportion of commercial cooking in local anthropogenic emissions was systematically accessed by the amended simulations driven from the SMAT-CE Tool under $Case_{on}$, $Case_{cc}$ and $Case_{an}$ (Fig. S12).

The annual contributions of commercial cooking to $PM_{2.5}$ concentrations at RG and SG were 1.23 and $1.27 \mu\text{g}/\text{m}^3$, respectively. Interestingly, the contribution exhibited obvious differences in seasons due to the corporate influence of seasonal monsoon climate and local commercial cooking emissions. Because of the prevailing northerly winds in autumn and winter (Fig. S11(e), Fig. S11(g)) and the intensive emissions in the eastern and northern Ronggui, the contribution of commercial cooking to $PM_{2.5}$ in autumn ($1.37 \mu\text{g}/\text{m}^3$) and winter ($1.70 \mu\text{g}/\text{m}^3$) at RG was significantly higher

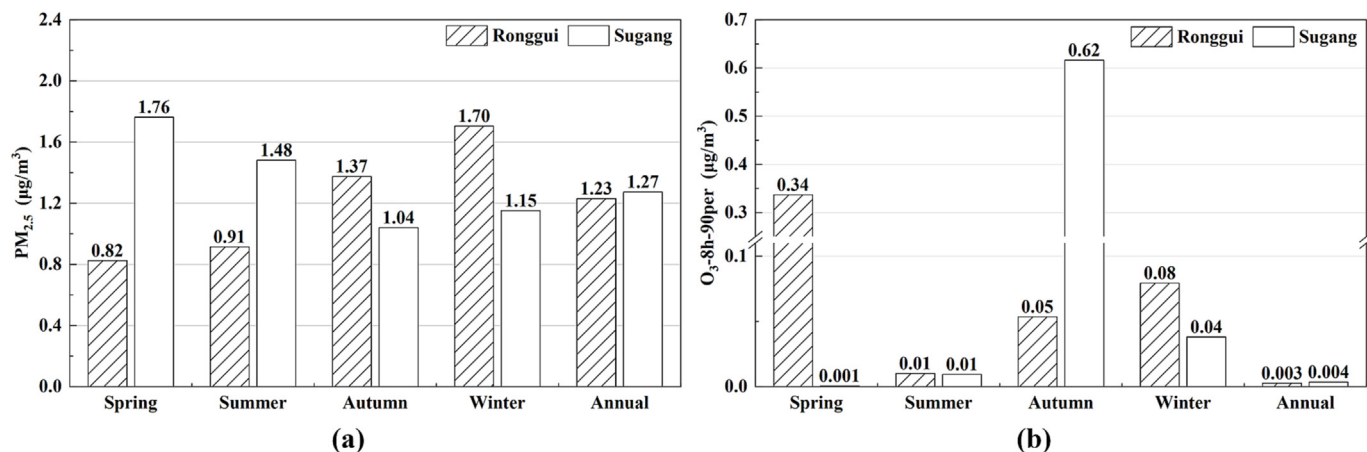


Fig. 5. Seasonal and annual contribution concentrations of commercial cooking to PM_{2.5} (a) and 90th percentile of the daily maximum 8-h average O₃ (O₃-8h-90per) (b) in Shunde district that obtained by subtracting the corresponding concentrations of Case_{on} from Case_{cc}.

than that in spring (0.82 µg/m³) and summer (0.91 µg/m³). However, an opposite trend was shown at SG, where the contribution in spring and summer was slightly higher than that in autumn and winter because southerly and easterly winds prevail in spring and summer (Fig. S11(b), Fig. S11 (d) and commercial cooking emissions are higher in these two directions around SG. Similar seasonal differences also occurred in the contribution proportion of commercial cooking in local anthropogenic emissions to PM_{2.5} as shown in Fig. S12. The annual and seasonal contribution proportion of commercial cooking at two stations ranged between 20 % - 28 % and 19 % - 28 %, respectively, sharing a similar result with that in the case study of Patras, Greece conducted by Siouti et al. (2021), in which the cooking organic aerosol contributed 14 % of PM_{2.5} in the city center, proving a non-negligible impact of local commercial cooking emissions on PM_{2.5}. On the contrary, the contribution of commercial cooking to O₃

concentrations was nearly negligible in both two sites. On the one hand, as the aforementioned explanation, Shunde was a typical regional emission-affected area (You et al., 2017), implying less contribution of local emissions on O₃ formation; on the other hand, the source profiles of SPECIATE 5.2 used in this simulation were insufficient to represent the emission characteristics of local commercial cooking because there were significant differences in the emission characteristics of the oil fumes between Western and Chinese cooking activities, especially commercial cooking. As such, the variation of local commercial cooking emissions had less effect on its O₃ formation.

Fig. 6(a) showed the hourly contribution of local commercial cooking emissions to annual and seasonal ambient PM_{2.5} concentrations. A peak contribution was predicted at 18:00–20:00 (Beijing time) in all four seasons, which was consistent with the peak dining time (18:00–20:00, Beijing

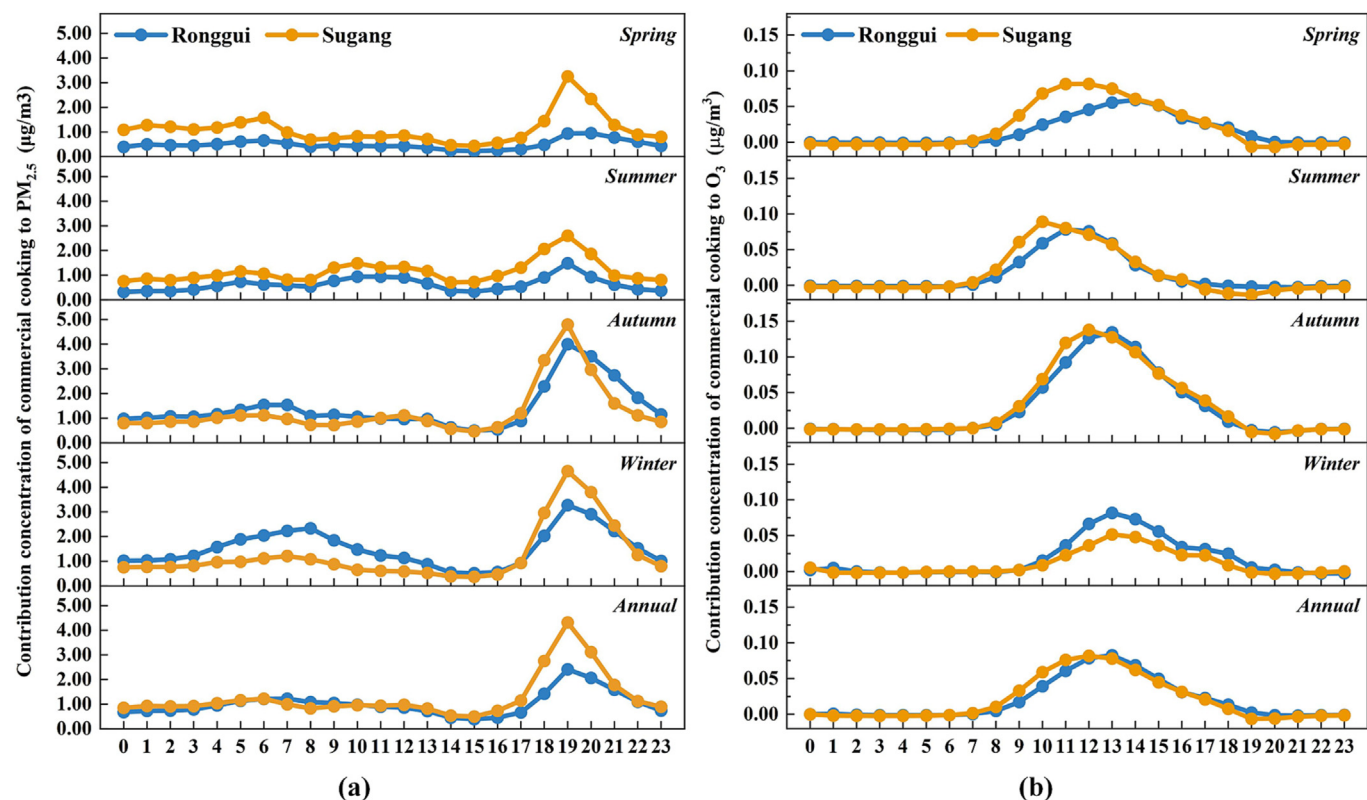


Fig. 6. Seasonal and annual hourly contribution concentration of commercial cooking to ambient PM_{2.5} (a) and O₃ (b).

time) of restaurants in Fig. 4(c). The annual contributions to $PM_{2.5}$ at RG and SG also peaked at 18:00–20:00 (Beijing time), with the highest contribution of $4.00 \mu\text{g}/\text{m}^3$ and $4.80 \mu\text{g}/\text{m}^3$, respectively. Besides, it was found that the intensive emissions at lunchtime of restaurants and breakfast time of canteens in Fig. 4(c) did not cause a corresponding obvious increase in $PM_{2.5}$ concentration, which is probably because of the relatively favorable atmospheric diffusion conditions at midday. The hourly contribution of commercial cooking emissions to both seasonal and annual O_3 was much lower than that to $PM_{2.5}$, with the highest contribution only at $0.083 \mu\text{g}/\text{m}^3$ (RG) and $0.082 \mu\text{g}/\text{m}^3$ (SG), respectively, furtherly proving that the impact of local commercial cooking emissions on O_3 is ignorable overall.

The spatial distribution of local commercial cooking emission contribution to ambient $PM_{2.5}$ and O_3 was illustrated in Fig. 7(a-e) and (f-j). The distribution of high contribution to $PM_{2.5}$ was consistent with the spatial allocation of commercial cooking emissions in Fig. 3, which was concentrated around each monitoring station, suggesting that the commercial cooking emissions exert a more noticeable impact on its nearby area. Among different monitoring stations, there was little difference in the contribution to $PM_{2.5}$ concentrations. The overall contribution concentration in winter was higher than that in other seasons, with the highest contribution of $5.93 \mu\text{g}/\text{m}^3$, which may be related to the poor diffusion condition in winter. As for the O_3 , the emissions of commercial cooking in the southern and eastern Shunde contributed the most in spring, summer and winter, respectively. However, compared with $PM_{2.5}$, the distribution of high commercial

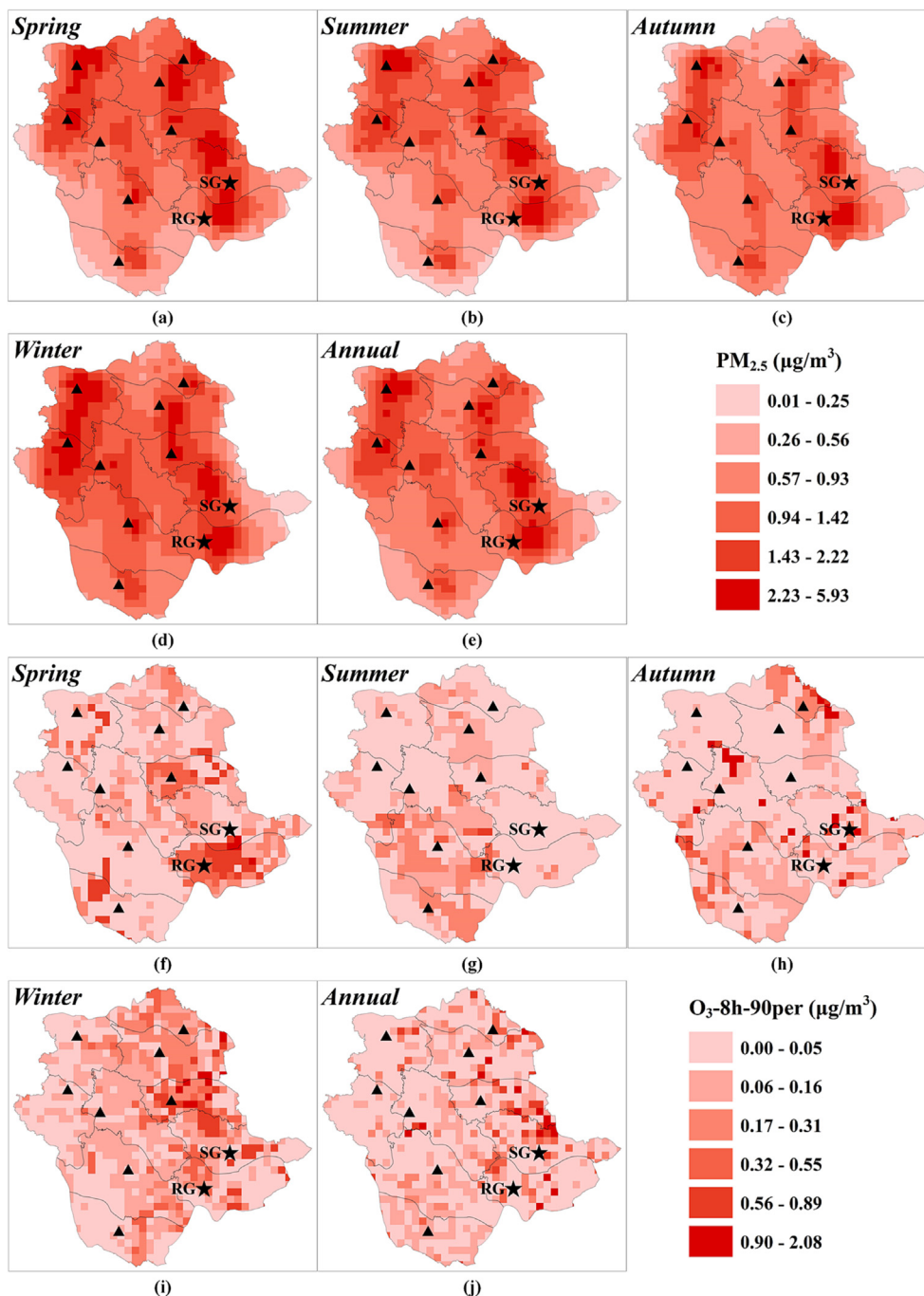


Fig. 7. Seasonal and annual spatial distribution of local commercial cooking contribution to ambient $PM_{2.5}$ (a-e) and 90th percentile of the daily maximum 8-h average O_3 (O_3 -8h-90per) (f-j).

cooking contribution to O₃ was more dispersed and the maximum grided contribution was 2.08 µg/m³. These results again emphasized the local impact of commercial cooking emissions on PM_{2.5} concentrations, whereas its impact on O₃ was not as significant as on PM_{2.5} in this study.

4. Conclusions

In this case study, the potential of using online oil fumes monitoring data together with the official statistical and investigation data to develop a high-resolution emission inventory of commercial cooking was demonstrated for the first time. The OOFM data-assisted emission inventory was then implemented into the WRF-CMAQ coupled modeling to verify the improvement effect and accordingly quantify the contribution of local commercial cooking emissions to ambient PM_{2.5} and O₃.

The OOFM data-assisted emission inventory can not only capture more detailed emission characteristics for commercial cooking but also be beneficial to improving simulation performance. The discrepancies in the emissions between our estimations and the legacy version reflected the well-developed catering industry and the rapid growth of the take-out industry. Regarding temporal-spatial variations, the major improvement in the study was to develop the temporal-spatial surrogates with a gridded resolution of 1 km at multi-temporal scales based on the realistic coordination of each restaurant and canteen and the OOFM data. High emissions were mainly agreed with block distributions around air monitoring stations. Different monthly, daily (within a week) and hourly variations were discovered for restaurants and canteens emissions, in which the low emissions of canteens during winter and summer vacations, the opposite weekend effect between restaurants and canteens and the beforehand emissions in the morning of both restaurants and canteens were all first reported. With the renewal of both emissions magnitude and temporal-spatial surrogates, the NMB and R of both PM_{2.5} and O₃ in the EL_{on}-based simulation scenario were generally improved, demonstrating the region-wide improvement on simulation with the application of OOFM and other realistic data. The simulation results proved a more pronounced impact of commercial cooking emissions on PM_{2.5} in nearby areas but a nearly negligible impact on O₃, indicating that targeted control measures should be implemented in specific regions to reduce the local commercial cooking emissions for continuous reduction of local PM_{2.5} concentrations.

However, there were still two limitations in our study. First, owing to the potential inaccuracy of OOFM measurement caused by the light-scattering principle, the use of OOFM data was limited to the statistics of working hours and the temporal variation of emissions, which was still not enough for a reliable emission inventory. The advanced application of OOFM data in inventory compilation, such as the use of corrected online oil fumes concentration by in-situ monitoring to estimate pollutant emissions directly, will further improve the estimate emissions. Second, the lack of a local model-ready VOCs source profile specifically for cooking emissions could be responsible for the low contribution of local commercial cooking to O₃. Hence, the compilation of this profile has been listed in our subsequent plan to further improve the performance of PM_{2.5} and O₃ simulation.

To the best of our knowledge, this is the first study to compile a high-resolution emission inventory and explore detailed emission characteristics of commercial cooking assisted with OOFM data, providing a new guide for future accuracy improvement of commercial cooking emission inventories. Our findings can be used as an important scientific basis for the emission reduction regulations on commercial cooking.

CRedit authorship contribution statement

Yingzhi Yuan: Conceptualization, Methodology, Software, Investigation, Writing - original draft and revise.

Yun Zhu: Resources, Writing - review, editing & revising, Supervision, Project administration, Data curation.

Che-Jen Lin: Writing - review, editing & revising, Data curation.

Shuxiao Wang: Resources, Writing - review & editing, Data curation.

Yanghong Xie: Resources, Project administration.

Haixian Li: Validation, Formal analysis, Visualization.

Jia Xing: Resources, Writing - review & editing, Data curation.

Bin Zhao: Writing - review & editing.

Mengmeng Zhang: Validation, Software.

Zhiqiang You: Formal analysis, editing.

Data availability

Data will be made available on request.

Declaration of competing interest

The authors declare that they have no known competing financial interests or personal relationships that could have appeared to influence the work reported in this paper.

Acknowledgments

This work was supported by the High-precision and Rapid Traceability Research of UAV clusters Projects of Core Technology Research Project in Shunde District, Guangdong Province, China (No. 2130218003008) and the Demonstration Application Project of Catering Oil Fume Emission Status, Air Quality Impact and Pollution Control in Shunde District, Guangdong Province, China (No. 440606-2022-07248). The authors sincerely thank Dr. Carey Jang (U.S. Environmental Protection Agency) for his assistance in the preparation and management of this paper. The views expressed in this paper are those of the authors alone and do not necessarily reflect the views and policies of the U.S. Environmental Protection Agency.

Appendix A. Supplementary data

Thirteen figures, five tables and additional information on (1) The structure of the online oil fumes monitoring system; (2) Method of estimating emissions of commercial cooking without OOFM data; (3) Calculation method of average number of stove heads, oil fumes gas rates and working hours corresponding to the restaurants/canteens of large, medium and small scale; (4) The calculation of SMAT-CE Tool; (5) Formulas of statistic indicators for the WRF-CMAQ validation; (6) Formulas of estimating contribution concentration and proportion of local commercial cooking emissions on ambient PM_{2.5} and O₃ were provided in the Supplementary Material.

References

- Cheng, S.Y., Li, L., Chen, D.S., Li, J.B., 2012. A neural network based ensemble approach for improving the accuracy of meteorological fields used for regional air quality modeling. *J. Environ. Manag.* 112, 404–414. <https://doi.org/10.1016/j.jenvman.2012.08.020>.
- Clean Air Asia, 2021. China Air 2021: air pollution prevention and control progress in Chinese Cities. <http://www.allaboutair.cn/uploads/soft/220411/ChinaAir2021.pdf> (accessed 2021-10-27).
- Crabbe, H., Beaumont, R., Norton, D., 1999. Local air quality management: a practical approach to air quality assessment and emissions audit. *Sci. Total Environ.* 235, 383–385. [https://doi.org/10.1016/S0048-9697\(99\)00241-7](https://doi.org/10.1016/S0048-9697(99)00241-7).
- ElSharkawy, M.F., Ibrahim, O.A., 2022. Impact of the restaurant chimney emissions on the outdoor air quality. *Atmosphere* 13, 261. <https://doi.org/10.3390/atmos13020261>.
- Evangelia, Siouti, Ksakousti, Skyllakou, Ioannis, Kioutsioukis, Giancarlo, Ciarelli, Pandis, Spyros N., 2021. Simulation of the cooking organic aerosol concentration variability in an urban area. *Atmos. Environ.* 265, 118710. <https://doi.org/10.1016/j.atmosenv.2021.118710>.
- Fang, T., Zhu, Y., Wang, S., Xing, J., Zhao, B., Fan, S., et al., 2021. Source impact and contribution analysis of ambient ozone using multi-modeling approaches over the Pearl River Delta region, China. *Environ. Pollut.* 289, 117860. <https://doi.org/10.1016/j.envpol.2021.117860>.
- Fengju, Lu., Boxiong, Shen, Peng, Yuan, Shuhao, Li, Yating, Sun, Xue, Mei, 2019. The emission of PM_{2.5} in respiratory zone from Chinese family cooking and its health effect. *Sci. Total Environ.* 654, 671–677. <https://doi.org/10.1016/j.scitotenv.2018.10.397>.
- Guangdong Food and Drug Administration, 2010. Implementing Rules of the Guangdong Food and Drug Administration on the Administrative Measures for Catering Service Licenses. (in Chinese) http://www.gd.gov.cn/zwgk/gongbao/2010/32/content/post_3362984.html (accessed 2012-10-08).

- Guenther, A.B., Jiang, X., Heald, C.L., Sakulyanontvittaya, T., Duhl, T., Emmons, L.K., et al., 2012. The Model of Emissions of Gases and Aerosols from Nature version 2.1 (MEGAN2.1): an extended and updated framework for modeling biogenic emissions. *Geosci. Model Dev.* 5, 1471–1492. <https://doi.org/10.5194/gmd-5-1471-2012>.
- Huang, R., Zhai, X.X., Ivey, C.E., Friberg, M.D., Hu, X.F., Liu, Y., et al., 2018. Air pollutant exposure field modeling using air quality model-data fusion methods and comparison with satellite AOD-derived fields: application over North Carolina, USA. *Air Qual. Atmos. Health* 11, 11–22. <https://doi.org/10.1007/s11869-017-0511-y>.
- Jiabin, Li, Yun, Zh.u., Kelly, James T., Jang, Carey J., Shuxiao, Wang, Adel, Hanna, et al., 2019. Health benefit assessment of PM_{2.5} reduction in Pearl River Delta region of China using a model-monitor data fusion approach. *J. Environ. Manag.* 233, 489–498. <https://doi.org/10.1016/j.jenvman.2018.12.060>.
- Jin, W.J., Zhi, G.R., Zhang, Y.Z., Wang, L., Guo, S.C., Zhang, Y., et al., 2021. Toward a national emission inventory for the catering industry in China. *Sci. Total Environ.* 754, 142184. <https://doi.org/10.1016/j.scitotenv.2020.142184>.
- Junichi, Kurokawa, Toshimasa, Ohara, 2020. Long-term historical trends in air pollutant emissions in Asia: Regional Emission inventory in ASia (REAS) version 3. *Atmos. Chem. Phys.* 20, 12761–12793. <https://doi.org/10.5194/acp-20-12761-2020>.
- Kabir, E., Kim, K.H., 2011. An investigation on hazardous and odorous pollutant emission during cooking activities. *J. Hazard. Mater.* 188, 443–454. <https://doi.org/10.1016/j.jhazmat.2011.01.113>.
- Kang, K., Kim, H., Kim, D.D., Lee, Y.G., Kim, T., 2019. Characteristics of cooking-generated PM₁₀ and PM_{2.5} in residential buildings with different cooking and ventilation types. *Sci. Total Environ.* 668, 56–66. <https://doi.org/10.1016/j.scitotenv.2019.02.316>.
- Lee, S.C., Li, W.M., Chan, L.Y., 2001. Indoor air quality at restaurants with different styles of cooking in metropolitan Hong Kong. *Sci. Total Environ.* 279, 181–193. [https://doi.org/10.1016/S0048-9697\(01\)00765-3](https://doi.org/10.1016/S0048-9697(01)00765-3).
- Li, J.X., Wang, Z.X., Chen, L.L., Lian, L.L., Li, Y., Zhao, L.Y., et al., 2020a. WRF-Chem simulations of ozone pollution and control strategy in petrochemical industrialized and heavily polluted Lanzhou City, Northwestern China. *Sci. Total Environ.* 737, 139835. <https://doi.org/10.1016/j.scitotenv.2020.139835>.
- Li, K., Jacob, D.J., Shen, L., Lu, X., De Smedt, I., Liao, H., 2020b. Increases in surface ozone pollution in China from 2013 to 2019: anthropogenic and meteorological influences. *Atmos. Chem. Phys.* 20, 11423–11433. <https://doi.org/10.5194/acp-20-11423-2020>.
- Li, X., Li, Y.L., Lu, X., Wang, Y.F., Zhang, H., Zhang, P., 2020c. An online anomaly recognition and early warning model for dam safety monitoring data. *Struct. Health Monit.* 19, 796–809. <https://doi.org/10.1177/1475921719864265>.
- Liang, X., Chen, L., Liu, M., Lu, Q., Lu, H., Gao, B., et al., 2022. Carbonyls from commercial, canteen and residential cooking activities as crucial components of VOC emissions in China. *Sci. Total Environ.* 846, 157317. <https://doi.org/10.1016/j.scitotenv.2022.157317>.
- Lin, P., Gao, J., He, W., Nie, L., Schauer, J.J., Yang, S., et al., 2021. Estimation of commercial cooking emissions in real-world operation: particulate and gaseous emission factors, activity influencing and modelling. *Environ. Pollut.* 289, 117847. <https://doi.org/10.1016/j.envpol.2021.117847>.
- Liu, Shuhan, Hua, Shenbing, Wang, Kun, Qiu, Peipei, Liu, Huanjia, Wu, Bobo, et al., 2018a. Spatial-temporal variation characteristics of air pollution in Henan of China: localized emission inventory, WRF/Chem simulations and potential source contribution analysis. *Sci. Total Environ.* 624, 396–406. <https://doi.org/10.1016/j.scitotenv.2017.12.102>.
- Liu, T.Y., Wang, Z.Y., Huang, D.D., Wang, X.M., Chan, C.K., 2018b. Significant production of secondary organic aerosol from emissions of heated cooking oils. *Environ. Sci. Technol. Lett.* 5, 32–37. <https://doi.org/10.1021/acs.estlett.7b00530>.
- Liu, Y., Fan, Z.P., You, T.H., Zhang, W.Y., 2018c. Large group decision-making (LGDM) with the participators from multiple subgroups of stakeholders: a method considering both the collective evaluation and the fairness of the alternative. *Comput. Ind. Eng.* 122, 262–272. <https://doi.org/10.1016/j.cie.2018.06.008>.
- Liu, X.Y., Li, N., Liu, S., Wang, J., Zhang, N., Zheng, X.B., et al., 2019. Normalization methods for the analysis of unbalanced transcriptome data: a review. *Front. Bioeng. Biotechnol.* 7. <https://doi.org/10.3389/fbioe.2019.00358>.
- Lu, X., Zhang, S.J., Xing, J., Wang, Y.J., Chen, W.H., Ding, D., et al., 2020. Progress of air pollution control in China and its challenges and opportunities in the ecological civilization era. *Engineering* 6, 1423–1431. <https://doi.org/10.1016/j.eng.2020.03.014>.
- Lu, F., Shen, B., Li, S., Liu, L., Zhao, P., Si, M., 2021. Exposure characteristics and risk assessment of VOCs from Chinese residential cooking. *J. Environ. Manag.* 289, 112535. <https://doi.org/10.1016/j.jenvman.2021.112535>.
- Militello-Hourigan, Ryan E., Miller, Shelly L., 2018. The impacts of cooking and an assessment of indoor air quality in Colorado passive and tightly constructed homes. *Build. Environ.* 144, 573–582. <https://doi.org/10.1016/j.buildenv.2018.08.044>.
- Richard, Burnett, Hong, Chen, Mieczyslaw, Szyzkowicz, Neal, Fann, Bryan, Hubbell, Arden, Pope C., et al., 2018. Global estimates of mortality associated with long-term exposure to outdoor fine particulate matter. *Proc. Natl. Acad. Sci. U. S. A.* 115, 9592–9597. <https://doi.org/10.1073/pnas.1803222115>.
- Robinson, E.S., Gu, P.S., Ye, Q., Li, H.Z., Shah, R.U., Apte, J.S., et al., 2018. Restaurant impacts on outdoor air quality: elevated organic aerosol mass from restaurant cooking with neighborhood-scale plume extents. *Environ. Sci. Technol.* 52, 9285–9294. <https://doi.org/10.1021/acs.est.8b02654>.
- Seaman, V.Y., Bennett, D.H., Cahill, T.M., 2009. Indoor acrolein emission and decay rates resulting from domestic cooking events. *Atmos. Environ.* 43, 6199–6204. <https://doi.org/10.1016/j.atmosenv.2009.08.043>.
- Shangguan, M.L., 2019. Research report on China's takeaway industry: first half of 2019 (in Chinese). *China Food* 20, 158. <https://doi.org/10.1016/j.chinafood.2019.07.073>.
- Shida, Sun, Luna, Sun, Geng, Liu, Chao, Zou, Yanan, Wang, Lin, Wu, et al., 2021. Developing a vehicle emission inventory with high temporal-spatial resolution in Tianjin, China. *Sci. Total Environ.* 776, 145873. <https://doi.org/10.1016/j.scitotenv.2021.145873>.
- Sturm, P.J., Sudy, C., Almbauer, R.A., Meinhardt, J., 1999. Updated urban emission inventory with a high resolution in time and space for the city of Graz. *Sci. Total Environ.* 235, 111–118. [https://doi.org/10.1016/S0048-9697\(99\)00198-9](https://doi.org/10.1016/S0048-9697(99)00198-9).
- Sun, C.Y., Zhao, L.Y., Chen, X., Nie, L., Shi, A.J., Bai, H.H., et al., 2022. A comprehensive study of volatile organic compounds from the actual emission of Chinese cooking. *Environ. Sci. Pollut. Res.* 29, 53821–53830. <https://doi.org/10.1007/s11356-022-19342-4>.
- Tan, Y.T., Mao, X.Q., 2021. Assessment of the policy effectiveness of Central Inspections of Environmental Protection on improving air quality in China. *J. Clean. Prod.* 288, 125100. <https://doi.org/10.1016/j.jclepro.2020.125100>.
- U.S. Environmental Protection Agency, Office of Air Quality Planning and Standards, Division Air Quality Analysis, Group Air Quality Modeling, Research Triangle Park North Carolina, 2007. Guidance on the use of models and other analyses for demonstrating attainment of air quality goals for ozone, PM_{2.5}, and regional haze. <https://nepis.epa.gov/Exe/ZyPURL.cgi?Dockey=P1009011.TXT> (accessed April 2007).
- Wang, X.F., Ji, X.G., 2020. Sample size estimation in clinical research from randomized controlled trials to observational studies. *Chest* 158, S12–S20. <https://doi.org/10.1016/j.chest.2020.03.010>.
- Wang, H., Zhu, Y., Jang, C., Lin, C.J., Wang, S.X., Fu, J.S., et al., 2015. Design and demonstration of a next-generation air quality attainment assessment system for PM_{2.5} and O₃. *J. Environ. Sci.* 29, 178–188. <https://doi.org/10.1016/j.jes.2014.08.023>.
- Wang, H., Xiang, Z., Wang, L., Jing, S., Lou, S., Tao, S., et al., 2018. Emissions of volatile organic compounds (VOCs) from cooking and their speciation: a case study for Shanghai with implications for China. *Sci. Total Environ.* 621, 1300–1309. <https://doi.org/10.1016/j.scitotenv.2017.10.098>.
- Wan-qing, He, Ai-jun, Shi, Xia, Shao, Lei, Nie, Tian-yi, Wang, Guo-hao, Li, 2020. Insights into the comprehensive characteristics of volatile organic compounds from multiple cooking emissions and aftertreatment control technologies application. *Atmos. Environ.* 240, 117646. <https://doi.org/10.1016/j.atmosenv.2020.117646>.
- Xiao, Q.Y., Geng, G.N., Xue, T., Liu, S.G., Cai, C.L., He, K.B., et al., 2022. Tracking PM_{2.5} and O₃ pollution and the related health burden in China 2013–2020. *Environ. Sci. Technol.* 56 (11), 6922–6932. <https://doi.org/10.1021/acs.est.1c04548>.
- Xing, L., Fu, T.M., Liu, T., Qin, Y., Zhou, L., Chan, C.K., et al., 2021. Estimating organic aerosol emissions from cooking in winter over the Pearl River Delta region, China. *Environ. Pollut.* 292, 118266. <https://doi.org/10.1016/j.envpol.2021.118266>.
- Xu, H., Ta, W., Yang, L., Feng, R., He, K., Shen, Z., et al., 2020. Characterizations of PM_{2.5}-bound organic compounds and associated potential cancer risks on cooking emissions from dominated types of commercial restaurants in northwestern China. *Chemosphere* 261, 127758. <https://doi.org/10.1016/j.chemosphere.2020.127758>.
- Xuehong, Zh.u., Hailing, Li, Jinyu, Chen, Feitao, Jiang, 2019. Pollution control efficiency of China's iron and steel industry: evidence from different manufacturing processes. *J. Clean. Prod.* 240, 118184. <https://doi.org/10.1016/j.jclepro.2019.118184>.
- Yang, W.Y., Chen, H.S., Wang, W.D., Wu, J.B., Li, J., Wang, Z.F., et al., 2019. Modeling study of ozone source apportionment over the Pearl River Delta in 2015. *Environ. Pollut.* 253, 393–402. <https://doi.org/10.1016/j.envpol.2019.06.091>.
- Yang, Lei, Zhang, Qijun, Zhang, Yanjie, Lv, Zongyan, Wang, Yanan, Wu, Lin, et al., 2021. An AIS-based emission inventory and the impact on air quality in Tianjin port based on localized emission factors. *Sci. Total Environ.* 783, 146869. <https://doi.org/10.1016/j.scitotenv.2021.146869>.
- You, Z.Q., Zhu, Y., Jang, C., Wang, S.X., Gao, J., Lin, C.J., et al., 2017. Response surface modeling-based source contribution analysis and VOC emission control policy assessment in a typical ozone-polluted urban Shunde, China. *J. Environ. Sci.* 51, 294–304. <https://doi.org/10.1016/j.jes.2016.05.034>.
- Yu, M.F., Zhu, Y., Lin, C.J., Wang, S.X., Xing, J., Jang, C., et al., 2019. Effects of air pollution control measures on air quality improvement in Guangzhou, China. *J. Environ. Manag.* 244, 127–137. <https://doi.org/10.1016/j.jenvman.2019.05.046>.
- Yu, X.N., Shen, L., Hou, X.H., Yuan, L., Pan, Y.P., An, J.L., et al., 2020. High-resolution anthropogenic ammonia emission inventory for the Yangtze River Delta, China. *Chemosphere* 251, 126342. <https://doi.org/10.1016/j.chemosphere.2020.126342>.
- Zhang, L., Zhao, T.L., Gong, S.L., Kong, S.F., Tang, L.L., Liu, D.Y., et al., 2018. Updated emission inventories of power plants in simulating air quality during haze periods over East China. *Atmos. Chem. Phys.* 18, 2065–2079. <https://doi.org/10.5194/acp-18-2065-2018>.
- Zhang, Z.R., Zhu, W.F., Hu, M., Wang, H., Chen, Z., Shen, R.Z., et al., 2021. Secondary organic aerosol from typical Chinese domestic cooking emissions. *Environ. Sci. Technol. Lett.* 8, 24–31. <https://doi.org/10.1021/acs.estlett.0c00754>.
- Zhao, X.W., Gao, Q., Yue, Y.J., Duan, L., Pan, S., 2018. A system analysis on steppe sustainability and its driving forces—a case study in China. *Sustainability* 10, 233. <https://doi.org/10.3390/su10010233>.
- Zhou, C.W., Fu, B.J., Wang, X.F., Yin, L.C., Feng, X.M., 2020. The regional impact of ecological restoration in the arid steppe on dust reduction over the metropolitan area in northeastern China. *Environ. Sci. Technol.* 54, 7775–7786. <https://doi.org/10.1021/acs.est.0c00017>.